



Comparison of Wind Speed-Up over Escarpments Derived from Numerical Modeling and Wind-Loading Codes

M. Soleimanian, F. Kilanehei*, M. M. Memarpour

Faculty of Engineering and Technology, Imam Khomeini International University, Qazvin, Iran

ABSTRACT: The most common lateral load is a wind load. The wind speed profile considers as an effective parameter to find the wind load. Topographic features such as escarpments and hills in flat area can significantly amplify wind speeds near the ground. The main aim of this study is to investigate the effects of the escarpment characteristics on the velocity profile and speed-up using the numerical model. At the first, the numerical model validated with the experimental results obtained through the wind tunnel of Texas University. Then, three kinds of escarpments with different slopes simulated and speed-ups obtained from the numerical model, wind tunnel, ASCE and Iran codes compared. The results of numerical model at the smaller slope showed better accordance with wind tunnel results. The effect of inlet velocity profile on the speed-up was numerically studied. Comparison of the results showed that the maximum speed-up using the velocity profile of Iran code is greater than using ASCE code. Finally, the effect of the escarpment height and width with the same slope on speed-up was investigated. The results showed that speed-up grows as the width and height increase; however, the effect of increasing the height is less.

Review History:

Received: 17 September 2018
Revised: 25 October 2018
Accepted: 25 October 2018
Available Online: 10 November 2018

Keywords:

Wind Velocity Profile
Speed-up
Escarpment
Numerical Modeling
Design Code

1- Introduction

Estimation of wind loads on structures plays a vital role in the design and construction of buildings. The wind speed profile considers as an effective parameter to find the wind load. The wind speed value grows with height; furthermore, topographical features such as hills and escarpments in flat open terrain have a quiet strong impact on wind speed profiles. The velocity increases dramatically near the crest, close to the ground surface, and as the height and distance from the crest is increasing, the velocity growth falls until it returns to the normal point. Topographical changes have been regarded as an important aspect in determining the velocity profile in the codes.

The necessity of recognizing governing phenomena, applying to the structures such as suspended bridges and tall buildings, makes the scientists use specific tools for flow simulation around such these areas. Analytical solution, experimental and numerical modeling could be used for simulating fluid flow. Owing to complex geometry of mentioned problems, analytical solution is not able to meet all the needs; therefore, it has almost been applied to special cases. Laboratory modeling also contains errors of

the scale change and measurement, additionally the use of which is limited as a result of some important drawbacks such as being time-consuming and high cost; nevertheless, it has been frequently utilized in special problems and verification of numerical models. Glanville [1] simulated airflow over a tall and steep escarpment by using a wind tunnel and compared the corresponding parameters and flow separation with the result of full-scale model measurements. Surface roughness effect on wind velocity and flow type over a 2D steep hill investigated by Cao and Tamura [2]. The research results indicate roughness reduction interact with both velocity and turbulence and decrease them. Four major wind loading standards, including, ASCE (2005), Japan (2004), AS/NZ (2002) and Euro (2002) were reviewed by Ngo and Letchford [3]. They compared the approaches to determine the topographic effect on speed profile, and summarized significant differences in several areas, as well as the different mathematical formulations employed. They also modeled seven types of escarpments and hills at the 1:1000 scale, focusing on the effects of surrounding surface roughness and slope angle of the feature [4]. With technology and computers science progression, the usage of numerical modelling remarkably increases as a powerful tool in solving complex equations. There was great progress in numerical techniques with the growth of the computing

Corresponding author, E-mail: kilanehei@eng.ikiu.ac.ir

power. Nowadays, computational fluid dynamics (CFD) has risen significantly to evaluate the wind flow over different regions and various structures. Bitsuamlak et al. [5], studied the effect of topography on the speed profile over different topography, includes hills, escarpments, Valleys and the other topographic features by the use of numerical model, wind tunnel, Canada code (NBCC) and measured data at the hilltop. The comparison of numerical model and measured data indicates unlike the downstream, the upstream measured data have an appropriate accordance. The effective properties of the velocity profile around a 2D hills was numerically investigated by using the LES turbulence model by Cao et al. [6]. The numerical model has been validated by experimental test, then effect of slope, roughness and turbulent flow around the hill is investigated. Huang and Xu [7] make a prediction of typhoon design wind speed and profile over buildings or bridges located in complex terrain. Abdi and Bitsuamlak [8] investigated the performance of five different turbulence models for estimating speed-up ratio and wake zones with complex topography which is simulated in two forms (2D and 3D). The entire of turbulence models can predict speed-up value ratio at the upstream hill with sufficient precision, the main downside is about recirculation and evaluation wake zones. Aini [9] studied flow pattern around the building with different height and different placement. He concluded that the tornados direction created between the buildings is entirely dependent on the height of buildings. Wind turbine systems have been studied by various researchers. In the study conducted by Khosravi et al. [10], the dynamic stability in a grid-connected wind turbine system based on Double Feed Induction Generator (DFIG) using the bifurcation theory has been investigated. Wind turbine wake flow fields were simulated using three actuator methods combined with LES model by Luo et al. [11]. The results of numerical simulation showed good agreement with the experimental results.

The study of the hybrid modelling approach with wind tunnel experiment for a region with complex topography was done by Jubayer and Hangan [12]. Numerical study of the downburst phenomenon over real topography were conducted by Abd-Elaal et al. [13]. The research showed that the hills' longitudinal width has the significant effects on speed-up factor and the vertical downburst wind speeds are intensified and produced an effective wind component on inclined surfaces at low heights. Ren et al. [14] investigated the characteristics of a wind field under a full-scale complex terrain, and established a rich wind field database to propose a prediction model for a spatial wind field. The mentioned researcher employed a LES turbulent model to simulate the behavior of the turbulent flow of the spatial wind field by using OpenFOAM 4.0. Reliability analysis on a high rise building with consideration of wind load was investigated by Zhang et al. [15]. All the most commonly applied reliability methods have been utilized in their analysis and compared based on the performance.

There has been a great deal of research dealing with the topographic effect on the velocity profile and speed-up by numerical and experimental modeling. However, the impact of the slope, height and shape of the escarpment have been less considered. In the present paper, the escarpment has been simulated with three different slopes models of 10%, 30%, 100% with cliff using ANSYS Fluent 17 software, then the results of numerical model have been compared

with wind tunnel data and ASCE and Iran codes procedures; furthermore, the effect of the escarpment shape and height on speed-up have been studied.

2- Code Methods

Wind speed profile in Iran and ASCE codes could be regarded as hourly mean and 3s average methods. The current study uses 3s average method. The topographic factor defined as the following:

$$\hat{M}_{zt} = \frac{\hat{V}_{zt}}{\hat{V}_z} = \frac{\hat{V}_z + \Delta\hat{V}_z}{\hat{V}_z} \quad (1)$$

Where \hat{V}_{zt} , is velocity at height z above local ground in exposure to topography, \hat{V}_z is velocity at height z in the front face of topography in flat area and $\Delta\hat{V}_z$ is difference between velocity on the topography and in the flat area. Escarpment features and other terrain exposure parameters are provided in Fig. 1.

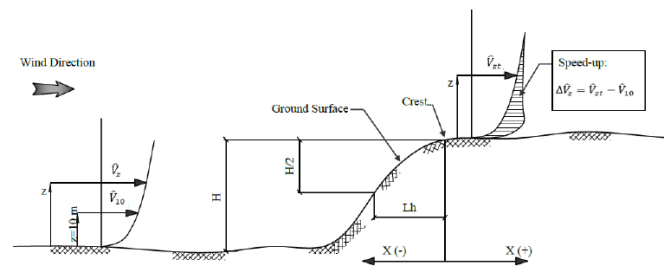


Figure 1. Characteristics of topographic features

In order to make a comparison between numerical simulation, and both the experimental results and codes, proportion of $\Delta\hat{V}_z$ to velocity \hat{V}_{10} indicating velocity of 10 meters height above the flat area is defined as dimensionless parameter:

$$\frac{\Delta\hat{V}_z}{\hat{V}_{10}} = \frac{\hat{V}_{zt} - \hat{V}_z}{\hat{V}_{10}} = \left(\frac{\hat{V}_{zt}}{\hat{V}_z} - 1 \right) \frac{\hat{V}_z}{\hat{V}_{10}} = (\hat{M}_{zt} - 1) \hat{M}_{zcat} \quad (2)$$

\hat{M}_{zcat} , is the ratio of speed at height z above the ground without any topography to the speed at a height of 10 m above the ground surface [3]. By the use of codes, \hat{M}_{zt} , will be obtained.

2- 1- ASCE code

Speed profile in open terrain defined by ASCE code as follows:

$$\bar{V}_z = \hat{b} \left(\frac{z}{10} \right)^{\hat{a}} V \quad (3)$$

Where V is based velocity, z is the height above the ground surface, \bar{V}_z is the velocity at height z and \hat{a} and \hat{b} are the coefficients which are presented in standards. The \hat{a} and \hat{b} in open terrain are equal to 0.086957 and 1.07 respectively [16]. Topographic factor is determined by:

$$M_{zt} = 1 + K_1 K_2 K_3 \tag{4}$$

K_1 which depends on topographic slope, types of topography, and terrain exposures given in Table 1. This term has the most significant impact on the speed up. According to Table 1, reduction of density and roughness, increase K_1 . K_2 and K_3 are the parameters for horizontal and vertical attenuation respectively, and determined by the following equations:

$$K_2 = \left(1 - \frac{|x|}{\mu L_h} \right) \tag{5}$$

$$K_3 = e^{-\gamma z / L_h} \tag{6}$$

Where the distance x and the length L_h are defined in Fig. 1. Both γ and μ depend on topographic types and exposure that given in Table 1. For the slopes either greater than 25% or $H/L_h > 0.5$, speed-up impact does not change with slope further due to the windward separation bubble formation in front of the topographical feature, and thus L_h is replaced by $2H$ to determine K_1 , K_2 , and K_3 .

2- 2- Iran code

In Iran code, two regions (open and full density) defined and speed profile is determined as Equation 7 [17].

$$V_z = V \sqrt{C_e} = V \sqrt{\left(\frac{z}{10} \right)^{\hat{\alpha}}} \tag{7}$$

Where C_e is the exposure factor in ground surface and V is based wind speed. For gust speed 3-second, coefficient $\hat{\alpha}$ equals to 0.1. Topographic factor obtained from the Equation 8:

$$C_e^* = C_e \left\{ 1 + \Delta S_{\max} \left(1 - \frac{|x|}{K L_h} \right) e^{(-\alpha z / L_h)} \right\}^2 \tag{8}$$

C_e^* is the correction factor based on the hills and escarpments. ΔS_{\max} is relative speed-up factor on the crest and close to the surface. The relative speed-up, α and K that depend on the topography shape given in Table 2. Comparison between Equation 4 and 8 indicates that the factors of ASCE code K_1 , K_2 and K_3 respectively, are equal with ΔS_{\max} , $(1 - |x| / (K L_h))$ and $e^{(-\alpha z / L_h)}$ Iran code.

It should be noted that, if the slope is greater than 25% or $H/L_h > 0.5$, L_h will be replaced by $2H$ (as ASCE code).

Table 1. Parameters for speed-up in ASCE code

Parameters of velocity increase over hills and escarpment						
Hill shape	$K_1 / (H/L_h)$			γ	μ	
	exposure				Upwind of crest	Downwind of crest
	B	C	D			
2-D ridges (or valleys with negative H in $K_1 / (H/L_h)$)	1.3	1.45	1.55	3	1.5	15
2-D escarpment	0.75	0.85	0.95	2.5	1.5	4
3-D axi-symmetrical hills	0.95	1.05	1.15	4	1.5	1.5

Table 2. Parameters for speed-up in Iran code

Shape of hill or escarpment	ΔS_{\max}	α	K	
			X<0	X>0
2-D ridges (or valleys with negative H)	2.2 (H/Lh)	3	1.5	1.5
2-D escarpment	1.3 (H/Lh)	2.5	1.5	4
3-D axi-symmetrical hills	1.6 (H/Lh)	4	1.5	1.5

3- Numerical model

As mentioned, numerical simulation done by ANSYS Fluent software17. Fluent is multipurpose software, which has enough capabilities to simulate a wide range of problem such as fluid flow, heat transfer etc. The software discretized the governing equation based on the finite volume method (FVM). Fluent can also simulate different condition such as steady and unsteady flows, viscous and non-viscous flow, compressible and incompressible flow, two phases, turbulence etc.

3- 1- Governing equation and boundary condition

The basic equations of fluid flow are conservation of mass (continuity equation) and momentum conservation (Navier-Stock equation). These equations provide an exact time-dependent solution, which have been used in both laminar and turbulent flow. Most of the flows in nature and engineering problems are turbulent and the most important characteristic of which is the fact that velocity and pressure at a point fluctuate with time in a random manner making the prediction flow behavior impossible. Turbulence modelling is a method that eliminates non-significant fluctuation flow feature and replaced them by mean values. There are several methods using some specific alters which do not need the small-scale fluctuation simulation. The space average and time average Reynolds method is one of these techniques which leads to a close-set equation by defining extra expressions. Nowadays, Reynolds time integration method considers as a conventional approach, which widely use in engineering problems. By considering the parameters as time - averaged and fluctuating terms ($\bar{\phi} = \bar{\phi} + \phi'$), and averaging the equations over a proper period, Navier-Stocks converts to Reynolds equation. Continuity and Reynolds-Averaged Navier–Stokes equations are the following 9 and 10:

$$\frac{\partial(u_i)}{\partial x_i} = 0 \quad (9)$$

$$\frac{\partial(u_i)}{\partial t} + \frac{\partial}{\partial x_j}(u_i u_j) + \frac{1}{\rho} \frac{\partial P}{\partial x_i} = \frac{\partial}{\partial x_j} \left[\mu \left(\frac{\partial u_i}{\partial x_j} + \frac{\partial u_j}{\partial x_i} \right) - \overline{u_i u_j'} \right] + \frac{f_i}{\rho} \quad (10)$$

Where, P is pressure, t demonstrates time, f_i is body force, u_i is the velocity component in x, y and z direction, μ is viscosity, (u_i') is the velocity fluctuation parameter in i-direction and $(\overline{u_i u_j'})$ is Reynolds stresses terms which is the component of the total stress tensor in a fluid obtained from the averaging operation over the Navier–Stokes equations to account for turbulent fluctuations in fluid momentum. Equations 9 and 10, composed by continuity and momentum equations include four unknown terms u, v, w and P. Moreover, the Equation 10 has six unknown stress terms $(\overline{u_i u_j'})$; therefore, the Equations 9 and 10 are not closed set (the unknown parameters are more than equations) so it is unsolvable. In order to make a closed form, turbulence model defines the stress terms as known or calculable parameters. There are different turbulence models with different complexity and capabilities. In the present research to close Reynolds-Averaged equation, K-ε turbulence model is used. This model has become one of the most widely used turbulence models as it provides robustness and acceptable accuracy for a wide range of turbulent flows. The efficiency of the K-ε turbulence model for flow simulation over escarpment has been shown in previous studies. The K-ε

model uses two transport equations, to calculate turbulence flow properties including K turbulent kinematic energy and ε turbulent dissipation. The turbulent kinetic energy k, and its rate of dissipation ε, for this model are obtained by the following equations.

$$\rho \frac{\partial k}{\partial t} + \rho u_j k_j = \left(\mu + \frac{\mu_t}{\sigma_k} \right) k_j + G + B - \rho \epsilon \quad (11)$$

$$\rho \frac{\partial \epsilon}{\partial t} + \rho u_j \epsilon_j = \left(\mu + \frac{\mu_t}{\sigma_\epsilon} \right) \epsilon_j + C_1 \frac{\epsilon}{k} G + C_1 (1 - C_3) \frac{\epsilon}{k} B - C_2 \rho \frac{\epsilon^2}{k} \quad (12)$$

C_1 , C_2 , σ_k , σ_ϵ , and C_3 are experimental factors which respectively equal to 1.44, 1.9, 1, 1.3 and 0.9 [18].

Defining the appropriate boundary condition is one of the most important aspects of numerical modelling. Three types of boundary conditions, including velocity, output and wall have been used in this article. The velocity condition is the speed profile applied to the domain inlet, which is presented in codes (ASCE and Iran). The output boundary condition is an outflow with 100% flow rate. The other boundaries (bottom, top and walls domain) are defined as wall with zero shear stress.

4- Validation

The numerical model validated against the case study of Nego and Lechford and the results compared with both ASCE and Iran code. Researchers investigate seven experimental models with two types of topography (with the same height and different slopes) in Texas University wind tunnel. Width, height and length of the wind tunnel are respectively equal to 1.8, 1.2 and 17 meters, which shown in Figure 2. Four types of escarpment modelling with the slopes of 10%, 30%, 100% and cliff have been chosen. The experimental model results have been reported either with or without carpet, in this research it is considered without carpet. Escarpment height is 50 mm and the scale of which is 1:1000. Flow velocity measured along the centerline of the wind tunnel. V_{10} is the velocity at height of 10 meters above the ground surface considered 15 m/s. Width and height of the numerical model, were considered respectively 1.8 and 1.2 m as the wind tunnel, the length of the model is selected 13 m to reduce the runtime. The four models shown in Figure 2 placed five meters away from the inlet. The dimensions of the solution domain presented in Figure 3.

The mesh elements are tetrahedral and close to the bottom it is used smaller element and the grid dimension is increasing as it is getting away from the bottom. As mentioned, structured mesh was used to discretize the computational domain. In structured mesh, the dimensions of the elements are important for achieving proper accuracy and efficiency. The grid analysis was carried out for all the numerical models. In the following, the process and its results are presented for escarpment with 10% slope.

First stage: 160 elements in length, 20 elements in width and 25 elements in height

Second stage: 200 elements in length, 40 elements in width and 60 elements in height

Third stage: 260 elements in length, 60 elements in width and 90 elements in height

In order to obtain the number of necessary elements for

numerical analysis, the value of wind speed up with the different elements are determined and compared. As shown in Figure 4, the results of the second and third stages have

far few differences, and reduction of the grid size in the third stage, has no remarkable effects on the results; therefore, the number of third stage elements is used for numerical analysis.

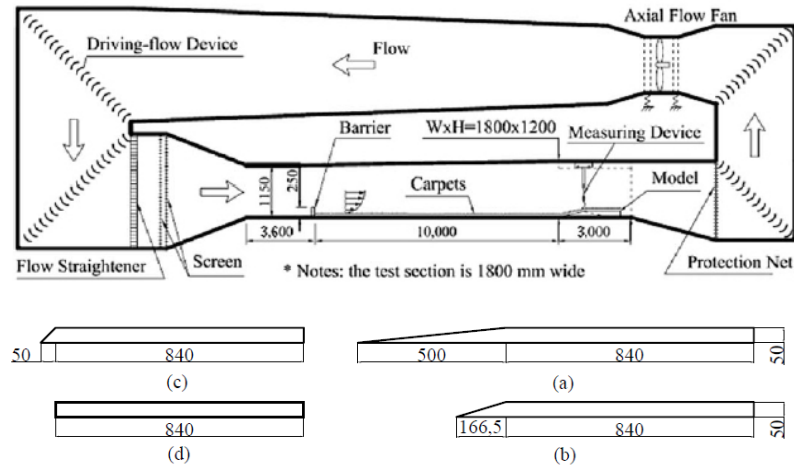


Figure 2. The wind tunnel of Texas University and topographic dimension a) 10% slope escarpment b) 30% slope escarpment c) 100% slope escarpment d) cliff [4]

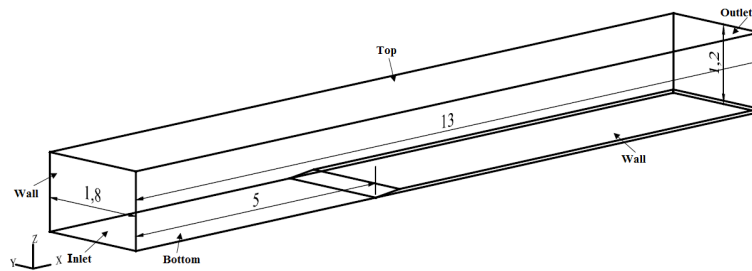


Figure 3. Dimension of numerical model

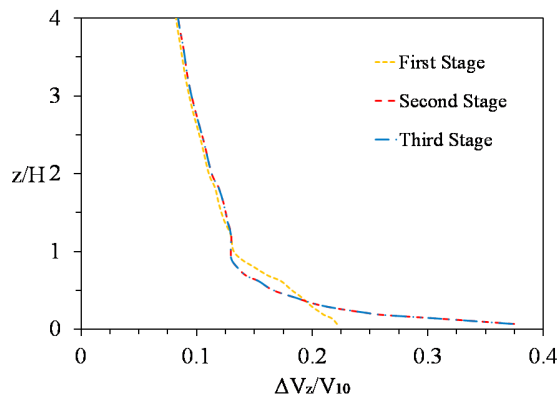


Figure 4. Comparison of speed-up profiles on the crest of the 10% slope escarpment with different grid dimensions

The velocity profiles in flat areas (before arriving to topography) are obtained by experimental; Iran and ASCE codes are shown in Figure 5, In order to get a better vision, x-axis and y-axis are made dimensionless by the use of the velocity in open smooth terrain at the height 10 meters and the escarpment height (50 mm). As shown in Figure 5, the results of ASCE and Iran codes are respectively at the upstream and downstream of the experimental wind tunnel results. The speed profile of the ASCE code is very consistent with wind tunnel data at the lower heights ($z/H < 1$). In order to evaluate the results, the numerical model evaluated by statistical parameter as follows:

$$RMSE = \frac{\sqrt{\sum (\phi_i^{co} - \phi_i^{ex})^2}}{\sum \phi_i^{ex}} .100 \quad (13)$$

Where ϕ_i the assessing value and subscripts ex and co are respectively the experimental and code results. Root-mean-square error (RMSE) both ASCE and Iran velocity profile between wind tunnel data are respectively equal to 29 and 35 percent. As it is shown, velocity profile of ASCE code has good agreement with experimental results in comparison with Iran code.

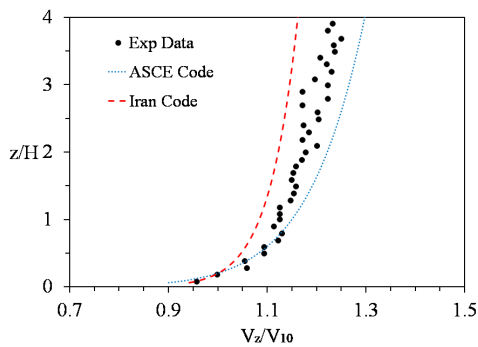


Figure 5. Velocity profile at the upstream side of the topography in open flat terrain by wind tunnel, ASCE code and Iran code

The speed-up obtained from numerical model, Iran code, ASCE code and wind tunnel located on the hilltop of 10% slope escarpment are presented in Figure 6. The results of numerical model and wind tunnel measured at the central line of the transverse axis (i.e. 0.9 m away and on the hilltop). To draw a comparison between the results of both Iran code and ASCE and numerical results, each of the velocity profile codes has been used as model input. Numerical results show discrepancies due to the different velocity profile as input Figure 5. The numerical results show better agreement at the lower heights ($0.5 < z/H < 1$) with ASCE code. Root Mean Square Error between the results of both ASCE code and the numerical model, and the results of wind tunnel are respectively equal to 16 and 19 percent, which show that the numerical model and code have great acceptance with experimental results; therefore, it indicated the perfect precision of numerical simulation. It can be deduced that the results of Iran code, are far different from the experimental

data at the lower heights (height ratio $z/H < 1.5$). RMSE between the results of both Iran code and numerical simulation and the results of wind tunnel data are respectively equal to 17 and 11 percent, which express perfect accordance between numerical model and the experimental results wind tunnel.

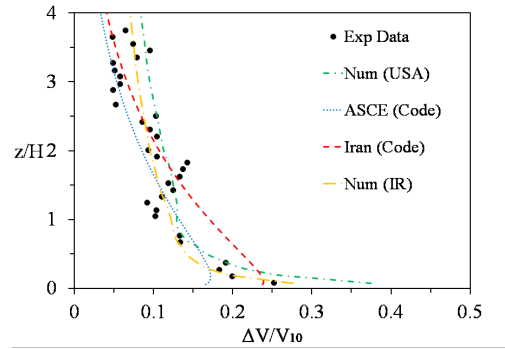


Figure 6. Speed-up profiles on the crest of the 10% slope escarpment

The deriving speed-ups through the numerical model, Iran code, ASCE code and wind tunnel on the crest of the 30% slope escarpment are shown in Figure 7. The 30% slope pattern is similar to 10% slope. RMSE between both ASCE code and numerical simulation and wind tunnel data are respectively equal to 34 and 25 percent. The values based on Iran code are shown 29 and 16 percent.

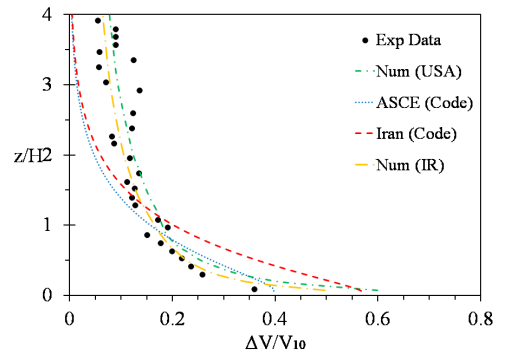


Figure 7. Speed-up profiles on the crest of the 30% slope escarpment

According to the statistical parameter, it will be deduced that the results of numerical simulation with the input of the velocity profile of Iran code, have more compatibility with experimental results; furthermore, the speed-up factor, which is predicted by numerical simulation in the 10% slope escarpment, has a great acceptance in comparison to 30% slope escarpment. The speed up profiles of the numerical model on the crest of the 10%, 30%, 100% slope escarpment and cliff are shown in Figures 8 and 9. Velocity profile using ASCE code employed as input data in numerical simulation.

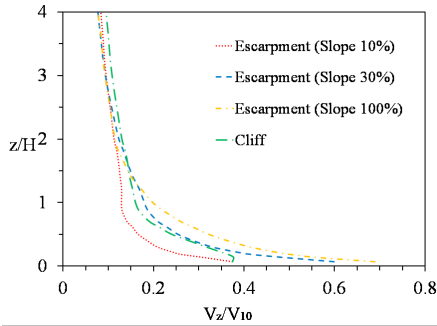


Figure 8. Speed-up profiles on the crest ($x=0$)

According to the Figure 8, the maximum speed-up becomes larger when the slope of escarpment increases. In the cliff simulation, the increased value of the velocity is smaller than 30% slope escarpment provided that the height ratio is less than 1.5. However, the increased value of velocity at the height ratio more than 1.5, is greater than the 100% slope.

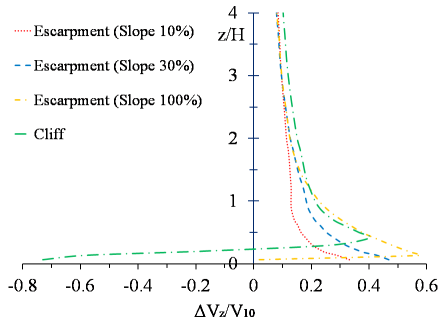
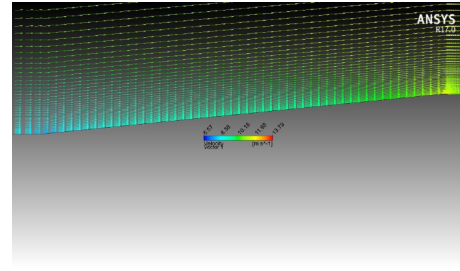


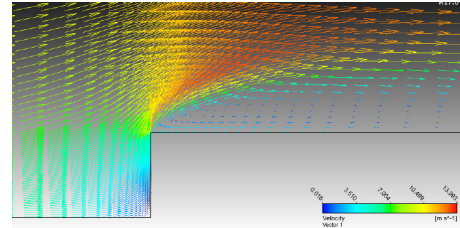
Figure 9. Speed-up profiles 10 meters away from the crest ($x=10$ m)

Figure 9 shows the speed-up profile 10 meters away from escarpment crest, pointing out the similar pattern on the crest. The flow pattern of cliff model and escarpment with 10% slope has been shown in Figure 10. Recirculation flow above the cliff zone, makes quiet small velocity at the heights smaller than 20 mm ($z/H < 0.4$).

In order to investigate the effect of inlet velocity profile on the speed-up factor, the numerical model results for the 10% and 25% slope escarpments with the input of Iran and ASCE velocity profile have been shown in Figure 11. According to the figure, the maximum speed-up velocity using Iran code is more than ASCE code in both of slopes.



(a)



(b)

Figure 10. Vectors over a) the cliff and b) escarpment with 10% slope

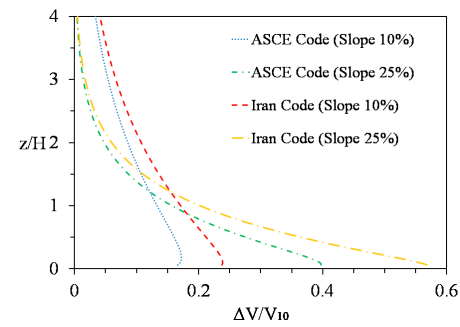


Figure 11. Comparison of speed-up velocity on the crest for 10% and 25% slope escarpments with Iran and ASCE inlet velocity profile

In the following, the influences of height and escarpment shape investigated on the speed-up factor.

5- Height effect

This section is about the evaluation of influence of height on the speed-up (with the same slope). The numerical model and ASCE code results of the 10% slope and with the heights 30, 50 and 70 mm, presented in Figure 12. It indicates that the both numerical model and code, speed-up factor increases when height grows and the numerical model results of all the three heights in small height ratios show, the speed-up values are equal, on the contrary the speed up values based on code are unequal. The mean of increased velocities by changing height from 30 mm to 50 mm and 50 mm to 70 mm are respectively 3.49 and 3.44 in numerical model, 2.06, and 1.62 percent in code. According to the numerical model results and codes, it deduced that in the case of a constant slope, the height increases do not affect significantly the speed-up.

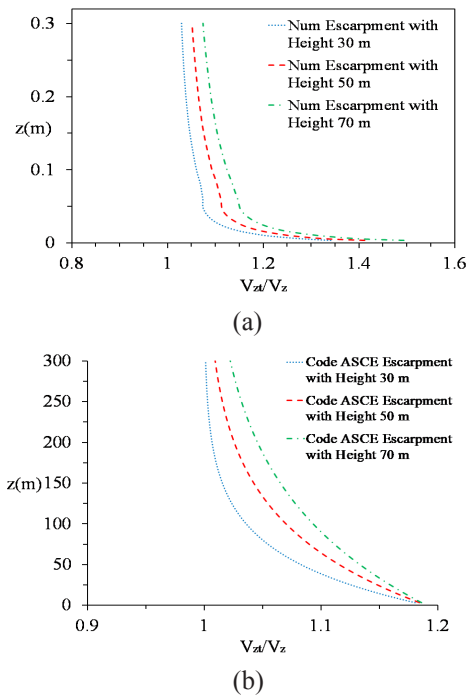


Figure 12. Influence of height on speed-up at the 10% slope escarpment a) numerical model b) ASCE code

6- Escarpment shape effect

The escarpment extended to full width in all the investigated models. Sometimes in flat area it can be seen, there is a strip escarpment (Figure 13). In order to evaluate the speed-up factor, strip escarpment simulated at four different conditions. Escarpment widths are respectively 0.2, 0.4, 0.6 and 0.8 m, the windward slope is 10 percent, and the lateral slope is 25 percent.

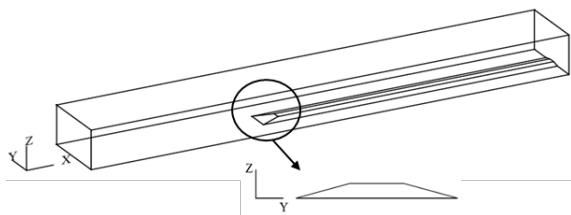


Figure 13. New shape of 10% slope escarpment

The speed-up simulated by numerical model at the escarpment crest and centerline are shown in Figure 14. Since the codes cannot consider the changes of escarpment width, the code results presented just for full width (1.8 m). According to the results, speed-up factor grows when the escarpment width increases. The speed-up growth is negligible in the small height ratios ($z/H < 0.5$), and as the height rises, the speed-up has a tangible increase. The mean increased velocities are from 0.2 m to 0.4 m, 0.4 m to 0.6 m, 0.6 m to 0.8 m and 0.8 m with full width respectively 10.23, 5.5, 4.9 and 18.72 percent. The maximum speed-up occurs at the full width condition. The full-width condition represents the 2D form of the escarpment considered in the codes. Thus, it concluded that in the case of the strip considering shape of

escarpment as a two-dimensional and full width brings about conservative results.

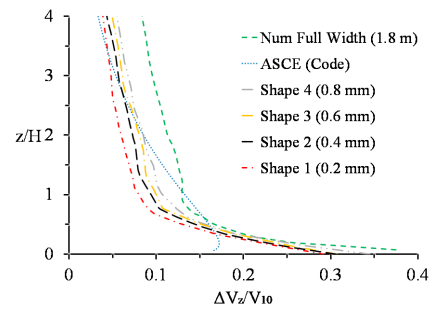


Figure 14. Speed-up profile with escarpment width change

7- Conclusion

In this research, the wind flow pattern over an escarpment numerically simulated and speed-ups derived from the numerical model, ASCE code, Iran code, and wind tunnel data compared. The results of the numerical model, ASCE and Iran codes, validated against Texas University wind tunnel data. The comparison of results demonstrates perfect accuracy and precision of the numerical model to simulate flow over an escarpment and determine speed-up. Furthermore, the results of numerical simulation by the use of Iran code velocity profile as the numerical model input have greater agreement with experimental data. The speed-up profile on the crest and 10 meters away from that with slopes of 10%, 30%, 100% and the cliff simulated. The results showed as the escarpment slope increasing, the maximum speed-up grows. The effect of inlet velocity profile on the speed-up studied too. The maximum speed-up using the velocity profile of Iran code is greater than using ASCE code. In the next steps, the effect of height (with the same slope) on speed-up investigated. The escarpment numerically simulated with 10% slope and heights of 30, 50 and 70 mm. The results indicate that the increases of the height do not have significant effect on the speed-up. Finally, escarpment shape investigated by escarpment change from strip to full width. The results indicate the speed-up rises when the width of the escarpment increases; consequently, the maximum speed-up occurs at the full width condition, or 2D form of the escarpment.

Nomenclature

English symbols

\hat{b}	3-s gust speed factor (ASCE code)
C_e	Exposure factor in ground surface
C_e^*	Correction factor based on the hills and escarpments
C_1, C_2, C_3, C_u	experimental factors
f_i	Body force ($i = x, y, z$)
G	Gravity acceleration
K	Factor to obtain C_e^* from table 2
K_1, K_2, K_3	Multipliers to obtain M_{zt} (in ASCE code)
K	Turbulent kinetic energy
L_h	Distance upwind of crest of escarpment to where the difference in ground elevation is half the height of the escarpment
\hat{M}_{zt}	Topographic factor (in ASCE code)
\hat{M}_{zt}	Topographic factor

\hat{M}_{zcat}	Ratio of (\hat{v}_z/\hat{v}_{10})
P	Pressure
t	Time
u_i	Velocity component (i= x, y, z) u_i
(\hat{u}_i')	Velocity fluctuation
$(u_i u_j)$	Reynolds stresses
\hat{V}_z^{zt}	Velocity at height z on topography zone
\hat{V}_z^z	Velocity at height z in flat area
\hat{V}_{10}^z	Velocity at 10 m height in flat area
\bar{V}_z	Velocity at height z (speed profile in ASCE code)
V_z	Based velocity
V_z	Velocity at height z (speed profile in Iran code)
X_z	Distance upwind or downwind of crest
z	Height above the ground surface (ASCE code)
Z	Height above the ground surface (Iran code)

Greek symbols

α	3-s gust speed power law exponent (ASCE and Iran code)
α	Factor to obtain C_e^* from table 2
Γ	Factor to obtain K_3 from table 1
ϵ	Dissipation rate
ΔS_{max}	Relative speed-up factor on the crest and close to the surface
$\Delta \hat{V}_z$	Difference between velocity on the topography and in the flat area. $\Delta \hat{V}_z = \hat{V}_z^{zt} - \hat{V}_z^z$
μ	Factor to obtain K_2 from table 1
μ	Viscosity
μ_t	Turbulent viscosity
ρ	Density
$\sigma_k, \sigma_\epsilon$	experimental factors
ϕ_i	Assessing value

Subscripts

co	Code result
ex	Experimental result
i, j, k	Component direction x, y, z
T	Turbulent
Z	Height of above ground surface
z_i	Height of above local ground in exposure to topography

References

[1] M. Glanville, K. Kwok, Measurements of topographic multipliers and flow separation from a steep escarpment. Part II. Model-scale measurements, Journal of wind engineering and industrial aerodynamics, 69 (1997) 893-902.

[2] S. Cao, T. Tamura, Experimental study on roughness effects on turbulent boundary layer flow over a two-dimensional steep hill, Journal of wind engineering and industrial aerodynamics, 94(1) (2006) 1-19.

[3] T. Ngo, C. Letchford, A comparison of topographic effects on gust wind speed, Journal of wind engineering and industrial aerodynamics, 96(12) (2008) 2273-2293.

[4] T.T. Ngo, C.W. Letchford, Experimental study of

topographic effects on gust wind speed, Journal of Wind Engineering and Industrial Aerodynamics, 97(9-10) (2009) 426-438.

[5] G. Bitsuamlak, T. Stathopoulos, C. Bédard, Numerical evaluation of wind flow over complex terrain, Journal of Aerospace Engineering, 17(4) (2004) 135-145.

[6] S. Cao, T. Wang, Y. Ge, Y. Tamura, Numerical study on turbulent boundary layers over two-dimensional hills—effects of surface roughness and slope, Journal of wind engineering and industrial aerodynamics, 104 (2012) 342-349.

[7] W. Huang, Y. Xu, Prediction of typhoon design wind speed and profile over complex terrain, Structural Engineering and Mechanics, 45(1) (2013) 1-18.

[8] D.S. Abdi, G.T. Bitsuamlak, Wind flow simulations on idealized and real complex terrain using various turbulence models, Advances in Engineering Software, 75 (2014) 30-41.

[9] A.H. Aini, Numerical Study of Flow Pattern in Buildings with Different Heights, Civil Engineering Journal, 2(3) (2016) 95-101.

[10] S. Khosravi, M. Zamanifar, P. Derakhshan-Barjoei, Analysis of Bifurcations in a Wind Turbine System Based on DFIG, Emerging Science Journal, 2(1) (2018) 39-52.

[11] X. Luo, Q. Li, S. Xiong, Z. Liu, Numerical Study of the Wake Flow of a Wind Turbine with Consideration of the Inflow Turbulence, Civil Engineering Journal, 4(8) (2018) 1907-1916

[12] C.M. Jubayer, H. Hangan, A hybrid approach for evaluating wind flow over a complex terrain, Journal of Wind Engineering and Industrial Aerodynamics, 175 (2018) 65-76.

[13] E.-S. Abd-Elaal, J.E. Mills, X. Ma, Numerical simulation of downburst wind flow over real topography, Journal of Wind Engineering and Industrial Aerodynamics, 172 (2018) 85-95.

[14] H. Ren, S. Laima, W.-L. Chen, B. Zhang, A. Guo, H. Li, Numerical simulation and prediction of spatial wind field under complex terrain, Journal of Wind Engineering and Industrial Aerodynamics, 180 (2018) 49-65.

[15] Y. Zhang, K. Yan, T. Cheng, Reliability Analysis of High Rise Building Considering Wind Load Uncertainty, Civil Engineering Journal, 4(3) (2018) 469-477.

[16] American Society of Civil Engineering. (ASCE), Minimum Design Loads for Buildings and Other Structures., (2010).

[17] Iranian National Building Code - 6th Chapter, Ministry of Housing and Urban Development, Department of Housing and Construction Office, Developing and Promoting National Regulations, (2013).

[18] Ansys, Inc. ANSYS FLUENT Theory Guide, ANSYS, Inc., (2010).

Please cite this article using:

M. Soleimani, F. Kilanehei, M. M. Memarpour, Comparison of Wind Speed-Up over Escarpments Derived from Numerical Modeling and Wind-Loading Codes , AUT J. Civil Eng., 3(1) (2019) 75-84.
DOI: 10.22060/ajce.2018.14996.5513



